Crossing a landslide area by a motorway

Núria M. Pinyol[1,2#], *Gaia* Di Carluccio[2,1], *José* Moya[1], *Josep M.* Bertran[3] and *Eduardo* Alonso[1,2 #]

[1]*Universitat Politècnica de Catalunya (UPC), Department of Civil and Environmental Engineering. Gran Capità, s/n 08034 Barcelona, Spain*
[2] *Centre Internacional de Mètodes Numèrics a l'Enginyeria (CIMNE). Jordi Girona, 1-3 08034 Barcelona,Spain*
[3] *Acciona Construcción. Departamento O.C. Zona Este. Plaça Europa 9-11, Torre Inbisa 10ª. 08908 L'Hospitalet de Llobregat. Barcelona. (SPAIN)*

[#] *nuria.pinyol@upc.edu*

ABSTRACT

A 1.5 km long stretch of a motorway built at midheigt of a valley eroded by an intermittent river, was almost completed in 2009. Budgetary restrictions led to a halt in construction. In the period 2009-2018, the motorway experienced severe damage, concentrated in three tributary shallow valleys, where the motorway was supported by compacted soil embankments.
The "valleys" were, in fact, ancient landslides reactivated by the weight embankment of the embankment. The damaged embankments were substituted by bridges supported by pile foundations designed to resist the thrust of the active landslides. The bridges were completed by pile walls to improve the stability of the landslides. The construction of the wide roadway platform (40 m) required excavations at the mountainside, embankments at the riverside, additional stabilizing measures by anchored resisting walls, and systematic drainage.
The miocene substratum is an irregular and heterogeneous set of conglomerate, sandstone, and claystone layers dipping 15-25º towards the river. The bedrock is covered by discontinuous quaternary clay and gravel formations.
The paper describes: a) The singular sheared surfaces with very low friction, located in claystones, which were responsible for the instabilities observed; they played a key role in designing the stabilizing measures; b) The complex water pressure distribution and its variability in time, a consequence of the geological structure of substratum and the procedure designed to reduce pore water pressures and c) The difficulties encountered to install permanent high capacity anchors and the evolution of anchoring loads.

Keywords: landslides; stabilizing measures; pile walls; drainage; anchored walls

1. Introduction

A 1.5 km long, 40 m-wide, 6-line motorway running parallel to a small stream (Fig. 1) was close to completion in 2009. However, budgetary restrictions led to a halt of construction works for a period of 9 years. When work resumed the platform showed, in several locations, major damage (Fig. 2).

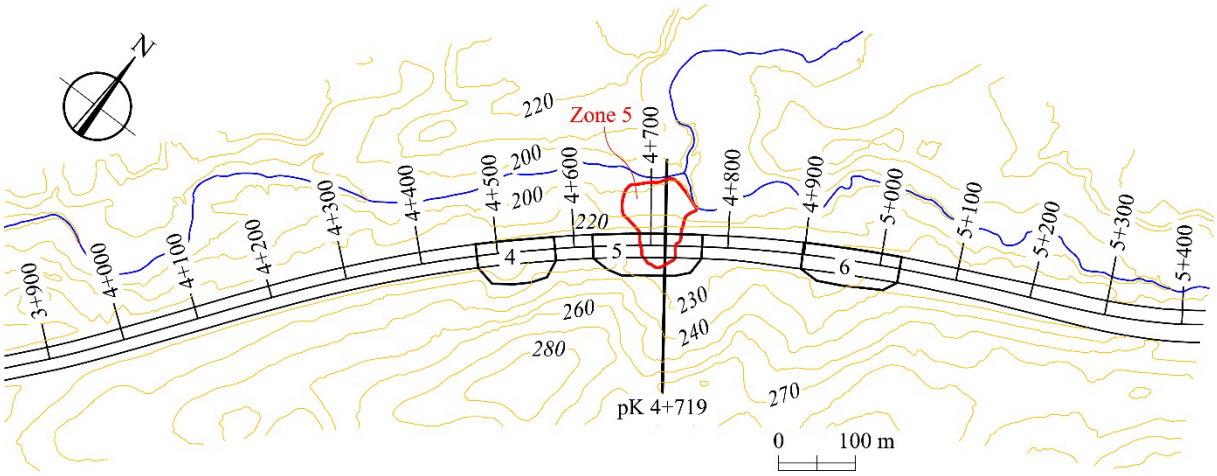

Figure 1. Plan view of the motorway. Location of the study zones.

Figure 2. Failure in "zone 5".

Figure 3 is a cross-section of the valley slope in the position shown in Figure 1 (chainage pK 4+719). The slope angle in the central-lower part of the valley is close to 12º. In other zones of the damaged motorway, the platform required excavation of the slope (mountain side) and an embankment in the river side. Valley slopes in the entire area range between 12º and 20º. This paper concentrates in the stability of the motorway in the 'zone 5'.

2. Geological and geotechnical information

Figure 3 shows a typical sequence of Miocene sand, sandstone, conglomerates and claystone layers in the area. They are tilted and dip angles match the topographic slope. The interpretation is that the topographic slope is a consequence of landsliding, probably occurred in quaternary times, triggered by the excavation of the river channel. A mantle of quaternary colluvial soils, -4 m thick in upper elevation and 6-7 m thick close to the river, covers the tertiary materials. Landslide failure surfaces follow contacts between hard (sandstones, conglomerates) and softer clayey layers, including the quaternary cover.

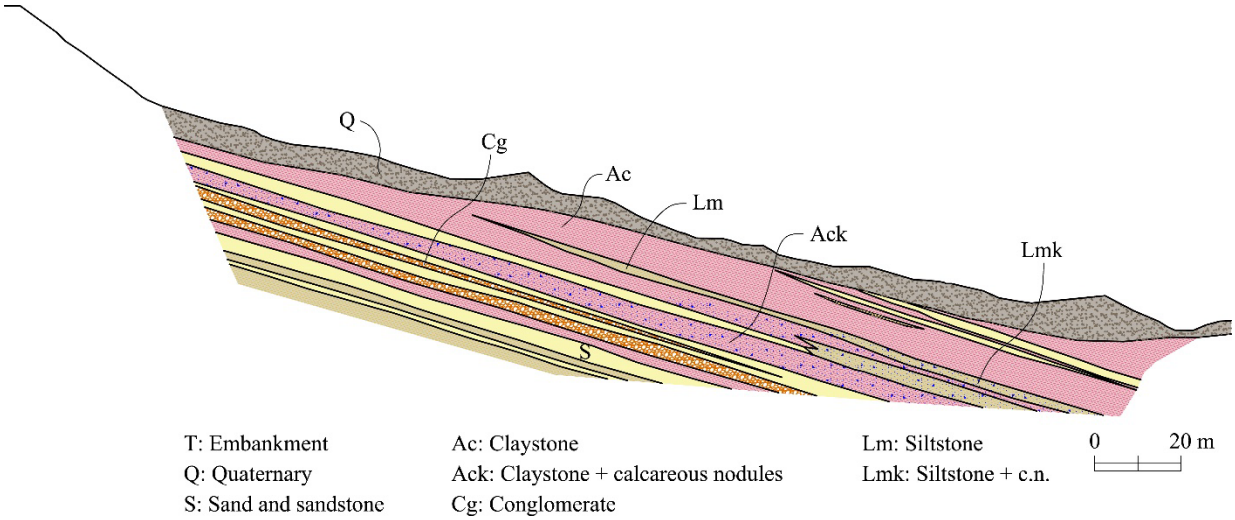

Figure 3. Central profile in zone 5.

Laboratory tests on samples of recovered cores and "in situ" dilatometers tests provided a picture of the geotechnical heterogeneity of the site. Unconfined compression strength for the sandstone and conglomerates ranges between 1 and 4.5 MPa. Claystone samples are weaker: 0.15 to 0.5 MPa. Fifteen pressuremeter tests were performed at depths varying from 13 to 32 m. Limit pressures ranging from 2.2 to 14 MPa provided an estimation of undrained strengths (0.4 to 2.5 MPa), a range of values that is reasonably consistent with the unconfined compression strengths. They provided also an estimation of the deformation moduli in the elastic range, E (35 to 650 MPa). If extreme values (too low and too high) are not accounted for, the E range reduces to 60 to 280 MPa.

Claystone samples had a low to medium plasticity (CL) and low water content. The friction angle determined in drained direct shear tests ranged from 20º to 25º.

Recovered cores in a significant amount of borings were examined to investigate the existence of slickensides, having in mind the past history of landslides of the valley slopes. Figure 4 is an example of a sheared surface in a stiff claystone. These features were often found.

Figure 4. Recovered specimen of striated shearing surface in a claystone material.

The excavation carried out in some locations offered the opportunity to examine in more detail the morphology of shearing surfaces. Figure 5 is a nice example. Figure 6 shows a sample of the surface with very distinct striation in the direction of a sliding motion. The sample was tested in a shear box by aligning the shearing surface with the shearing plane of the box. The measured residual friction angle reduced to 12º. The clay had, in this case, a high plasticity: $w_L = 46$, IP = 20.5.

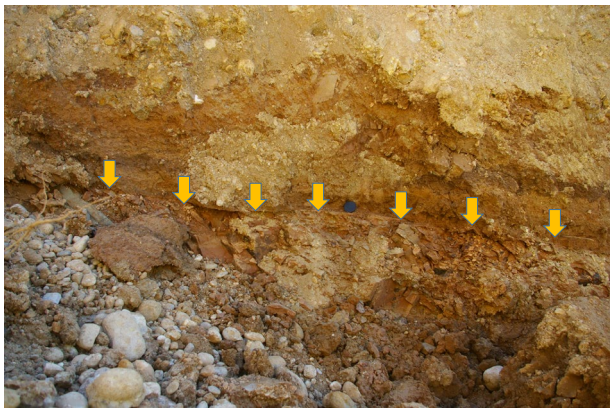

Figure 5. Shearing surface visible in an excavated face.

Figure 6. Recovered specimen showing the striated shearing surface indicated in Figure 5.

In ring shear tests on claystone samples, a residual friction of 22.8º was determined. It was realized that potential sliding surfaces in claystone contacts could exhibit a wide range of operating friction (12º-29º) because of the changes in plasticity. This variability of critical residual friction was introduced in finite element analysis (not reported here), performed for the design of stabilization measures, to check the safety of design alternatives.

3. Landslides and displacement monitoring

The original designers of the motorway decided to cross three small valleys, tributaries of the main river parallel to the road, using embankments and conventional surface drainage to evacuate the rainfall flows coming from higher elevations. The massive failure shown in Figure 2, in 'zone 5' (Fig. 1) and other local failures and deformations led to a detailed geomorphological evaluation of the entire area. The failure of section 5 was a reactivation of a landslide under the weight of the road embankments and, probably, a modification of hydrogeological conditions. Figure 1 shows an approximate contour of the landslide in Section 5. The head scarp was visible on the mountainside of the road and the slide toe reached the river channel.

Two more landslides were identified in 'Zone 4' and 'Zone 6' (Fig. 1). In these two zones the road platform had fissures and local failures of the embankment's slopes. The limits of the landslides were identified by field surveying.

A decision was taken to replace the three embankments with bridges whose abutments were located outside the limits of the landslides. Additional decisions were to support the bridge pillars on deep foundations and to stabilize the three landslides by pile walls (Figure 9).

The construction sequence adopted was (a) to build the foundation piles of pillars and abutments from the topographic surface, which included the damaged embankments; (b) partial excavation of the embankments between the location of pillars and between pillars and abutments; and (c) to stabilize the landslide by pile walls. Figure 7 shows the loading platforms in preparation for the installation of box girder beams. Figure 8 is a view of the completed bridge structure.

Figure 7. Construction of the piles loading platforms and box girder beams.

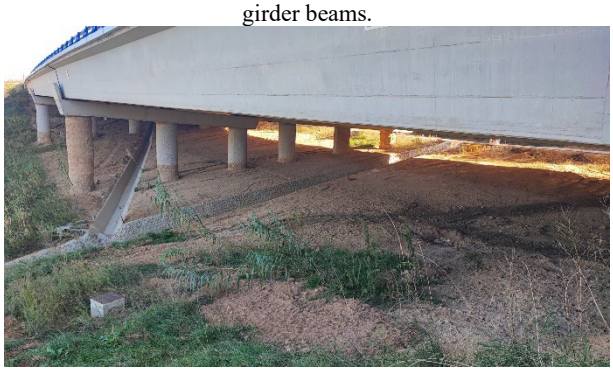

Figure 8. Bridge structure.

3.1. Inclinometer data

Figure 9 shows the position of inclinometer tubes S5.3, S5.2 bis, S5.2.1 and S5.5 in a transverse profile, centered in zone 5. Inclinometer's readings include systematic and random errors that should be accounted for. Mikkelsen (1996, 2003) and Stark and Choi (2008) describe the systematic errors and procedures to deal with them. The drift error, explained by deviations from verticality of accelerometer sensors, is the most frequent

one. Inclinometer data was systematically corrected in this study. Figures 10, 11 and 12 show measurements of inclinometer S5.2 and its replacement due to damage caused by construction works and excessive shearing displacements. The figures show a comparison of non-corrected and corrected displacements for three time intervals spanning the dates 27/05/2019 to 18/01/2021 (7.5 months). During this time the bridges were built in the previous locations of the embankments following the sequence of operations outlined above.

The landslide in zone 5 was active and moving down at a velocity of 13-14 mm/month (Fig. 10) at the beginning of comforting works.

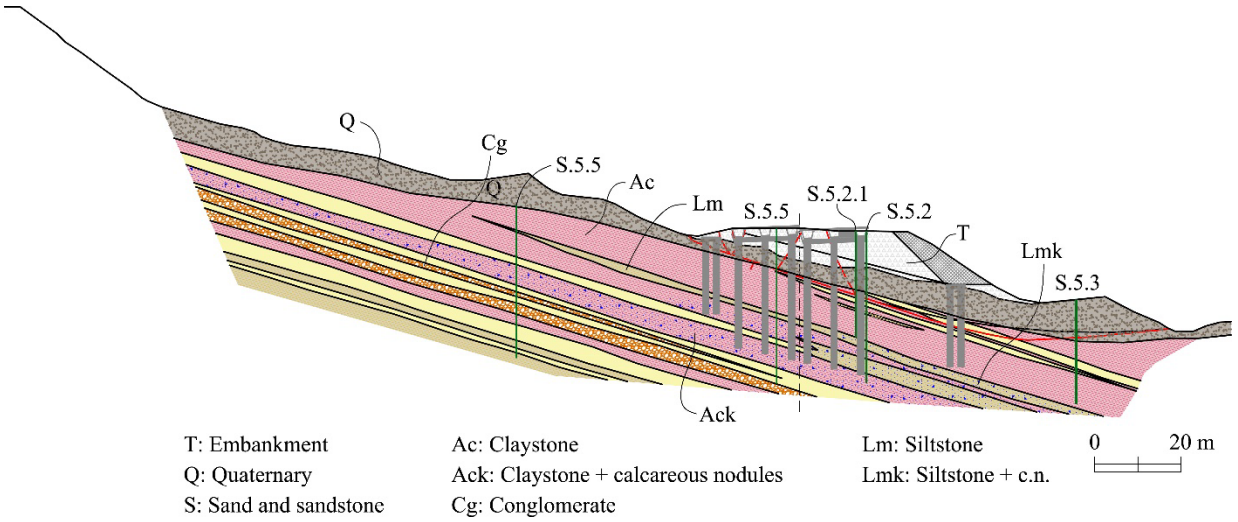

Figure 9. Central cross-section of Zone5 showing the original embankment, the piled bridge structure , the position of the two pile retaining walls and the position of piezometers

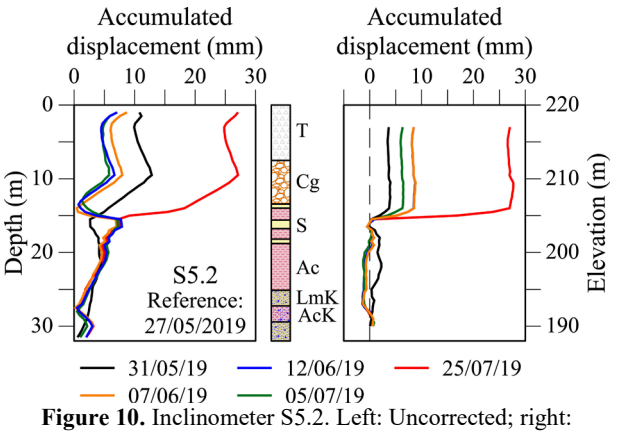

Figure 10. Inclinometer S5.2. Left: Uncorrected; right: corrected.

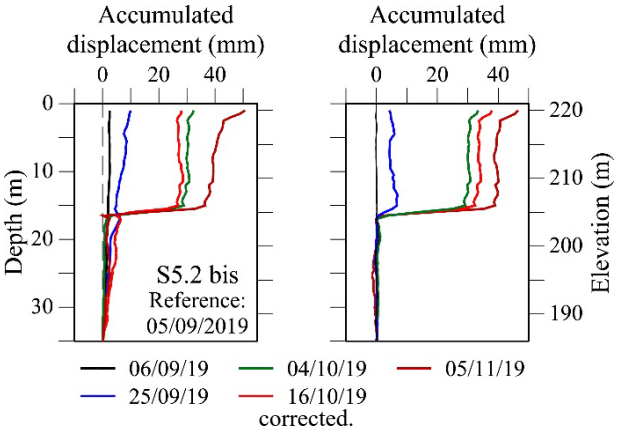

Figure 11. Inclinometer S5.2bis. Left: Uncorrected; right: corrected

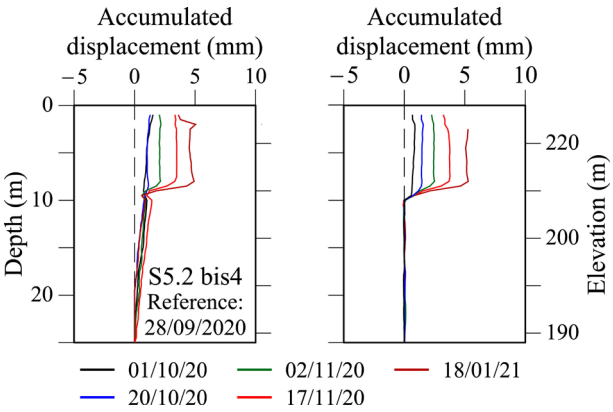

Figure 12. Inclinometer S5.2bis4. Left: Uncorrected; right: corrected

Figure 13 shows the evolution of landslide velocity during the period of bridge construction. The foundation piles and the removal of the embankment explain the reduction of landslide displacement rates. The landslide reached a very small creeping rate during the first months of 2022. The slide was further stabilized by building two pile walls in the position shown in Figure 9. The figure shows the position of the basal sliding surface, determined by inclinometer data, close to the contact between the quaternary layer and the miocene substratum. The upstream pile barrier was a protection from the potential instability of the quaternary deposits at higher elevations.

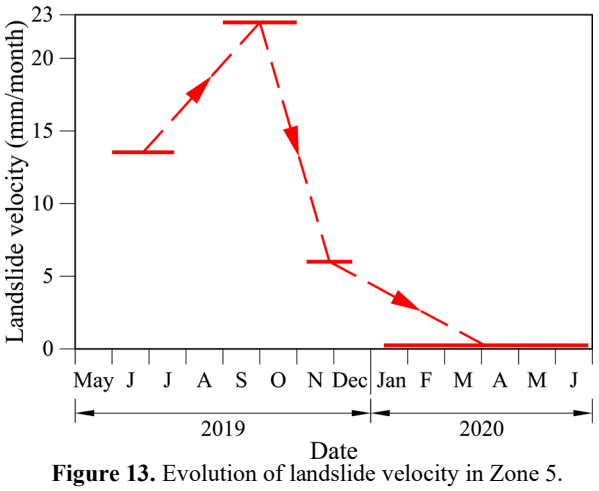

Figure 13. Evolution of landslide velocity in Zone 5.

4. Water pressure and drainage

Vibrating wire piezometers located in the vicinity of the inclinometer borings (Fig. 14) provided a continuous record of water pressures in the transition from the quaternary cover and the miocene substratum. Figure 14a (September 2020) shows high water pressures in the lower part of the quaternary layers and a significant reduction of pore water pressure in the upper miocene layers. This behavior may be explained by the high conductivity of sandstone strata below the quaternary soils. Water pressures reacted fast to precipitations. This is shown in Figure 14b, which shows a significant reduction in measured pressures few months later (January 2021). This behaviour and the sequence of pervious and impervious layers dipping towards the river suggested that the procedure to reduce water pressures in the entire unstable area crossed by the motorway was to communicate the layered structure by vertical drains. Hopefully, water will flow downwards toward pervious sandstone and conglomerate layers and, eventually, towards the stream bed. This procedure was deployed in the inter-zones between the bridges that were also affected by instabilities.

Figures 15, 16, and 17 show three zones that received this drainage treatment. The figures show also, in a cross-section, the support designed to stabilize the valley slope and the road platform, by means of anchored pile walls, rockfill walls, and anchor rows. The vertical drains, spaced 10 m, have a length of 20 m and a diameter of 150 mm. The performance of this drainage system is variable and can be explained by the heterogeneity and complex geometry of the miocene formation.

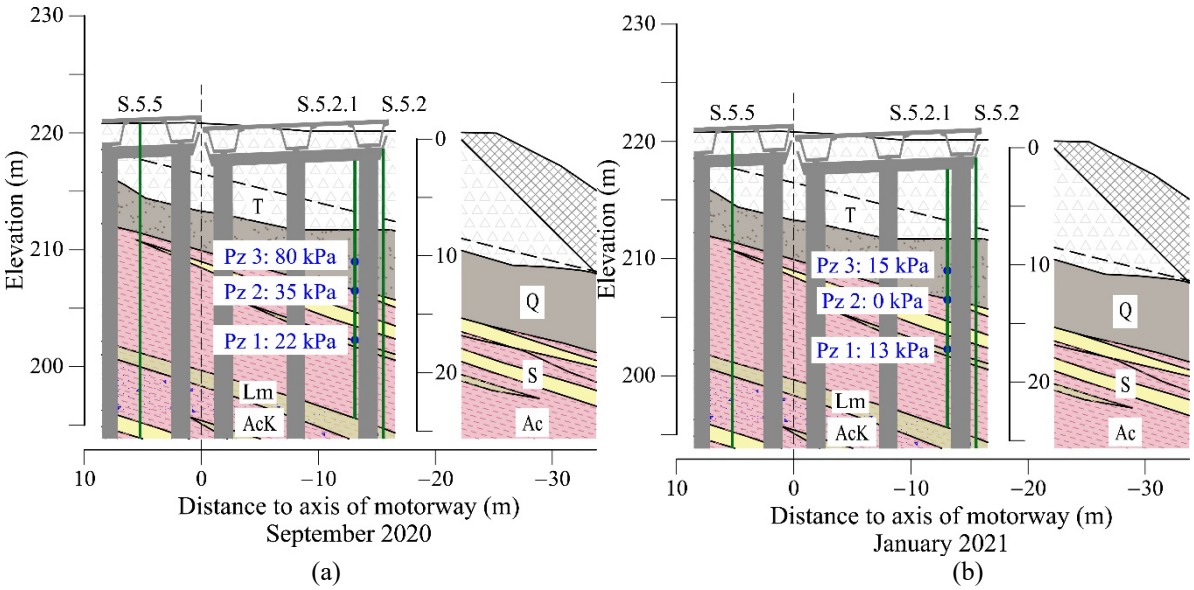

Figure 14. Piezometric measurements. (a) September 2020; (b) January 2021.

Figure 18 shows the measured water level in some drains protecting the road platform from pK 4+020 to pK 4+210. The first measurements (January 2022) indicated depths of free water close to 7 m. Two years later the measured depths ranged from 8.5 to 9 m. This range of levels is marked in Figure 15. In the road stretch from pK4+360 to 4+460 all the drains remained dry. This is a positive situation because of the instabilities observed originally in this section.

Figure 19 shows the measured water depths (February 2024) in drains installed in sections pK4+550 to pK4+660. This is a critical location because of the slope failures triggered by the excavations (mountain side) performed during the initial construction of the motorway. The recently recorded water depths in drains vary between 14 m, in half of the protected section, to 5.50 – 7.50 m in the second half (50 m long). This is marked in Figure 16. Overall, the effect of the vertical drains is estimated as a positive contribution to the stability of the road platform.

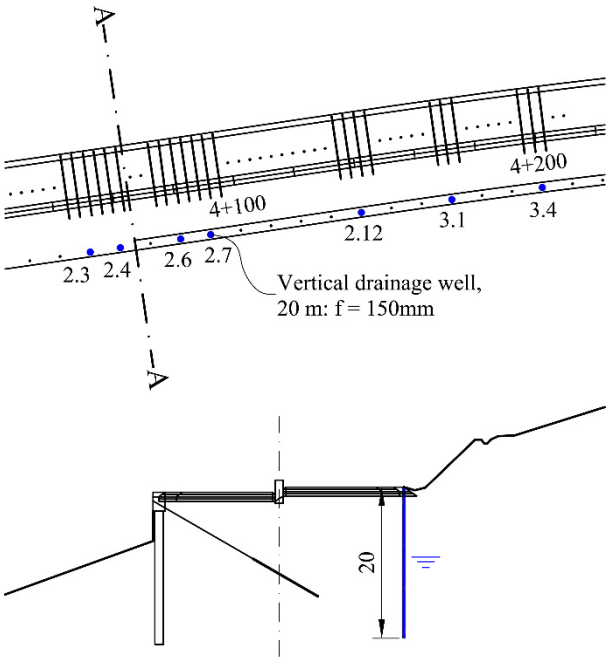

Figure 15. Pile wall and vertical drains between pK 4+020 and pK 4+210. Plan view and cross-section A-A.

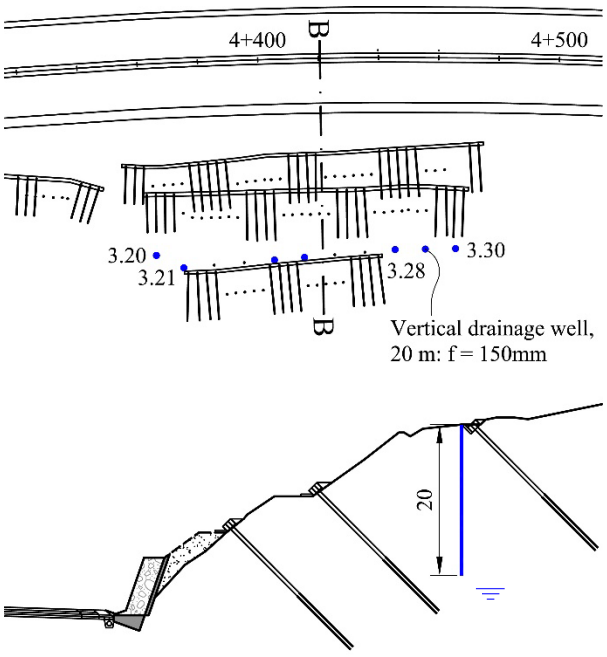

Figure 16. Rockfill wall, anchors and vertical drains between pK 4+360 and pK 4+460. Plan view and cross-section B-B.

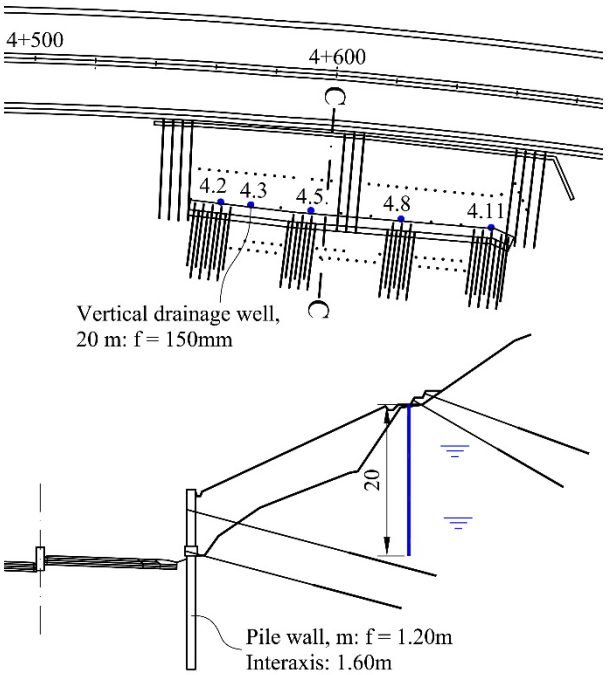

Figure 17. Anchored pile wall, anchors and vertical drains between pK 4+550 and pK 4+660. Plan view and cross-section C-C.

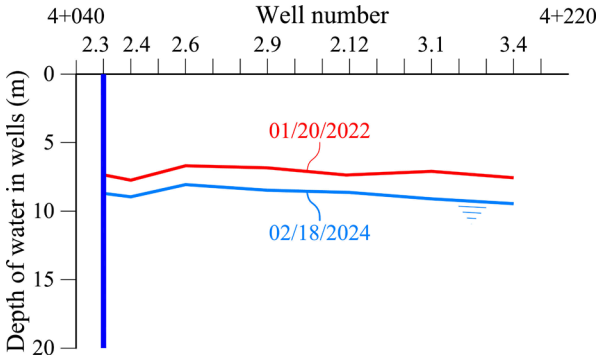

Figure 18. Water depth measured in drainage wells, at two times, in the zone between pK 4+020 and pK 4+210.

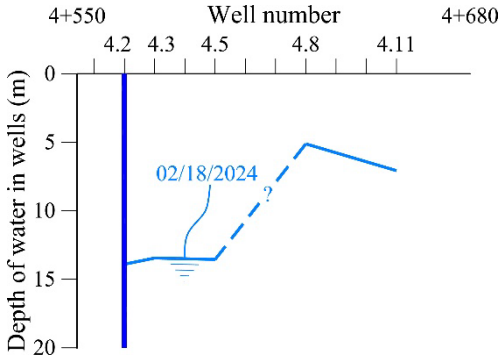

Figure 19. Water depth measured in drainage wells, in February 2024, in the zone between pK 4+550 and Pk 4+660

5. Anchors

The anchors shown in Figures 15, 16, and 17, and also in other locations, are of a 'permanent' type. Essentially, this is achieved through long-term protection of the high-strength cables from corrosion. In the anchoring zone (bulb), this is achieved by inserting an impervious tube protection between the borehole wall and the set of cables. A (smooth) steel tube was selected for this purpose. Preliminary pull-out loading tests indicated a failure of the 'adhesion' between the steel tube and the cement injection. The "adhesion" concept is somewhat misleading because the shear strength developing at the interface between the steel tube and the surrounding hardened cement grout is dominated by a frictional strength that is controlled by the normal stress to the interface and therefore, to a large extent, by the dilatancy of the steel-grout contact. Pressurized grout injection also contributes to increasing the available friction at interfaces. The problem was solved by welding corrugated bars (Figure 20) to the protection tubes (Figure 21).

Figure 20. Corrugated bars welded to the protective tubes of the grouted bulb of anchors

Figure 22 shows the evolution of the applied anchor loads in two different zones. In Figure 22a, the anchor lading was applied in two steps in a time interval of 60 days. A small to moderate reduction in the load is considered correct. This was the case for the monitored anchors. However, a proper diagnosis would require a much longer monitoring time. Maximum anchoring loads were set at 60 % of the limiting tensile strength of the steel cables to account for any potential increase of the required stabilizing anchor, although this does not seem likely in the future in view of the measured response so far.

6. Concluding remarks

In general terms, the 1.5 km long motorway mentioned in this paper was located on an unstable valley slope. The active landslides identified could take place at any time, in geological terms, and in any location. The slopes are unstable because the layered sequence of claystones and sandstones dips towards the eroding river channel. Dip angles of strata (15-20º) are similar to the topographic inclination of the slopes and, in addition, measured residual friction in claystone samples and striated sheared surfaces range between 12º and 20º. Moreover, positive pore water pressure, associated with natural water flow toward the river channel, contributes to instability.

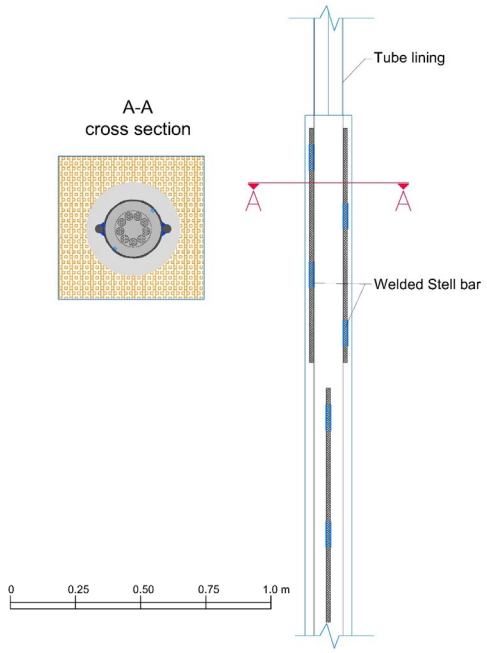

Figure 21. Design of the injected bulb protection of permanent anchors.

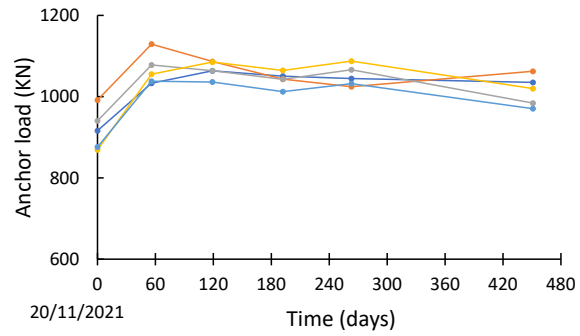

(a)

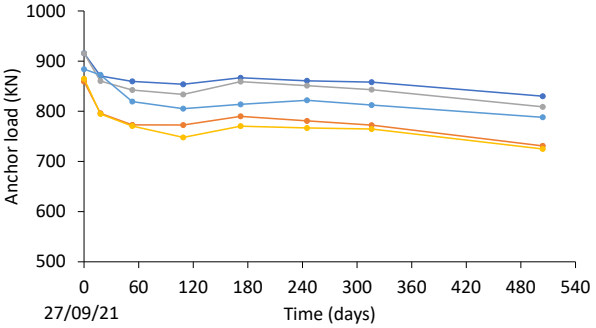

(b)

Figure 22. Evolution of anchoring loads in a few anchors installed in two zones of the unstable area: a) After a two-step application of the design load, the anchor load is essentially maintained after 16 months od monitoring. b) Moderate decay of anchor load in a different zone.

The stabilizing works mentioned (piles, pile walls, rockfill walls, drains, anchors) required an extense computational work that remains outside the focus of this paper. The main aspects described are:

- The singularity of sheared surfaces of very low friction in the sequence of miocene sandstones, conglomerates, and stiff claystones. They played a critical role in the process of designing comfort measures. In addition, they are difficult to find in site investigations.
- Failure to identify existing active landslides led to an inadequate design of embankment structures that added weight to the landslides, moved with the slide, and eventually collapsed.
- Substituting the embankments with bridges led to a stable solution for the road platform. Pile barriers stabilized the active landslides.
- Vertical drains connecting the layered geological structure of pervious and impervious levels reduced and even suppressed pore water pressures.
- The solution to protect anchor bulbs must guarantee a dilatant behavior between the hardened grout and the protection “envelope” of the injected anchored length.

7. References

Mikkelsen, E. “Ground displacement measurement”. In: Turner A.K. and Schuster R.L. (Eds.) Landslides. Investigation and Mitigation. Transportation Research Board, National Research Council, USA. Special Report 247. Chapter 11 Field instrumentation. 1996. pp. 282-295.

Mikkelsen, E. “Advances in inclinometer data analysis”. Symposium on Field Measurement in Geomechanics, Oslo, September, 2003. 13 p.

Stark, T.D., Choi, H. “Slope inclinometers for landslides”. Landslides, 5, pp 339-350. 2008.